

Synthesis, structure and catalytic activity of ruthenium diaminodiphosphine complexes

Wai-Kwok Wong,^{*,a} Xiao-Ping Chen,^a Jian-Ping Guo,^a Yong-Gui Chi,^a Wei-Xiong Pan^{a,b} and Wai-Yeung Wong^a

^a Department of Chemistry, Hong Kong Baptist University, Waterloo Road, Kowloon Tong, Hong Kong, P.R. China. E-mail: wkwong@hkbu.edu.hk

^b Department of Chemistry, Tsinghua University, Beijing, 100084, P.R. China

Received 1st August 2001, Accepted 2nd January 2002

First published as an Advance Article on the web 21st February 2002

The reaction of *N,N'*-bis[*o*-(diphenylphosphino)benzylidene]-1,2-diaminoethane (L^2) with one equivalent of $RuCl_2(PPh_3)_3$ in dichloromethane at room temperature gave *trans*- $RuCl_2(PPh_3)(\kappa^3-L^2)$ **2** in high yield. When refluxed in toluene in air, **2** was converted quantitatively to *trans*- $RuCl_2(\kappa^4-L^2)$ **3**. When treated with one equivalent of hydrogen peroxide in chloroform, **2** was oxidized to *trans*- $RuCl_2(PPh_3)(\kappa^3-L^3)$ **4**, in which the pendant phosphine has been oxidized to a phosphine oxide. Complex **4** can be further oxidized with another equivalent of hydrogen peroxide to *trans*- $RuCl_2(PPh_3)(\kappa^3-L^4)$ **5**, in which the amino group *trans* to PPh_3 has been oxidized to an imino group. When treated with excess hydrogen peroxide in ethanol, **3** was oxidized to *trans*- $RuCl_2(\kappa^4-L^5)$ **6**, in which the diamino moiety $[-N(H)CH_2CH_2N(H)-]$ has been oxidized to a conjugated diimino moiety $(-N=CHCH=N-)$. The solid-state structures of **2**, **4**, **5** and **6** were ascertained by X-ray crystallography. Catalytic studies show that **2** is an effective catalyst for the oxidation of alkanes, alkenes and alcohols with air or *tert*-butyl hydroperoxide. Experimental evidence suggests that free radicals are probably involved in the catalytic oxidation processes.

Introduction

Diamino-, diimino- and diamidodiphosphine ligands are very versatile ligands. These ligands exhibit very rich coordination chemistry and, depending on the reaction conditions, can behave as bridging, bi-, tri- and tetradentate ligands.^{1–8} Recently, there has been considerable interest in the preparation and chemistry of transition metal complexes with chiral diamino-, diimino- and diamidodiphosphine ligands^{9–18} as they have been shown to be effective catalysts for asymmetric hydrogen transfer reactions,¹² epoxidation,^{13,14} cyclopropanation¹⁵ and allylic alkylation.^{16–18} *N,N'*-bis[*o*-(diphenylphosphino)benzylidene]-1,2-diiminoethane (L^1 , see Chart 1) and *N,N'*-bis[*o*-(diphenylphosphino)benzylidene]-1,2-diaminoethane (L^2) are amongst the very first non-chiral diimino- and diaminodiphosphines to be synthesized.⁷ However, there have been relatively few studies on the chemistry and catalytic activities of their transition metal complexes as compared to their chiral analogues. We have reported the synthesis of *trans*- $RuCl_2(\kappa^4-L^1)$ and *trans*-

$RuCl_2(\kappa^4-L^2)$, and shown that they are effective catalysts for the hydrogenation of acrylic acid to propionic acid.⁵ Here, we describe the synthesis and reactivity of the novel complex *trans*- $RuCl_2(PPh_3)(\kappa^3-L^2)$, prepared *via* the reaction of $RuCl_2(PPh_3)_3$ with L^2 . Catalytic studies show that *trans*- $RuCl_2(PPh_3)(\kappa^3-L^2)$ is an effective catalyst for the oxidation of alkanes, alkenes and alcohols with air or *tert*-butyl hydroperoxide.

Results and discussion

Synthesis and characterization of ruthenium complexes

At room temperature in dichloromethane, $RuCl_2(PPh_3)_3$ reacted with one equivalent of L^1 and L^2 to give *trans*- $RuCl_2(\kappa^4-L^1)$ **1**⁵ and *trans*- $RuCl_2(PPh_3)(\kappa^3-L^2)$ **2**, respectively, in high yield (Scheme 1). The structure of **2**, which was ascertained by X-ray crystallography (Fig. 1), is similar to that of the recently reported *trans*- $RuCl_2(PPh_3)(\kappa^3-(1R,2R)-L^6)$ $\{(1R,2R)-L^6 = (1R,2R)-N,N'$ -bis[*o*-(diphenylphosphino)benzylidene]-1,2-di-

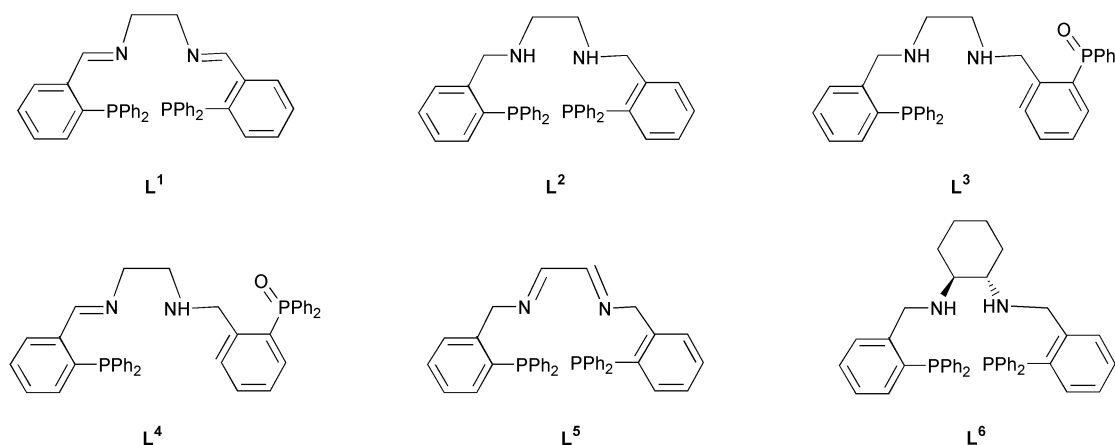
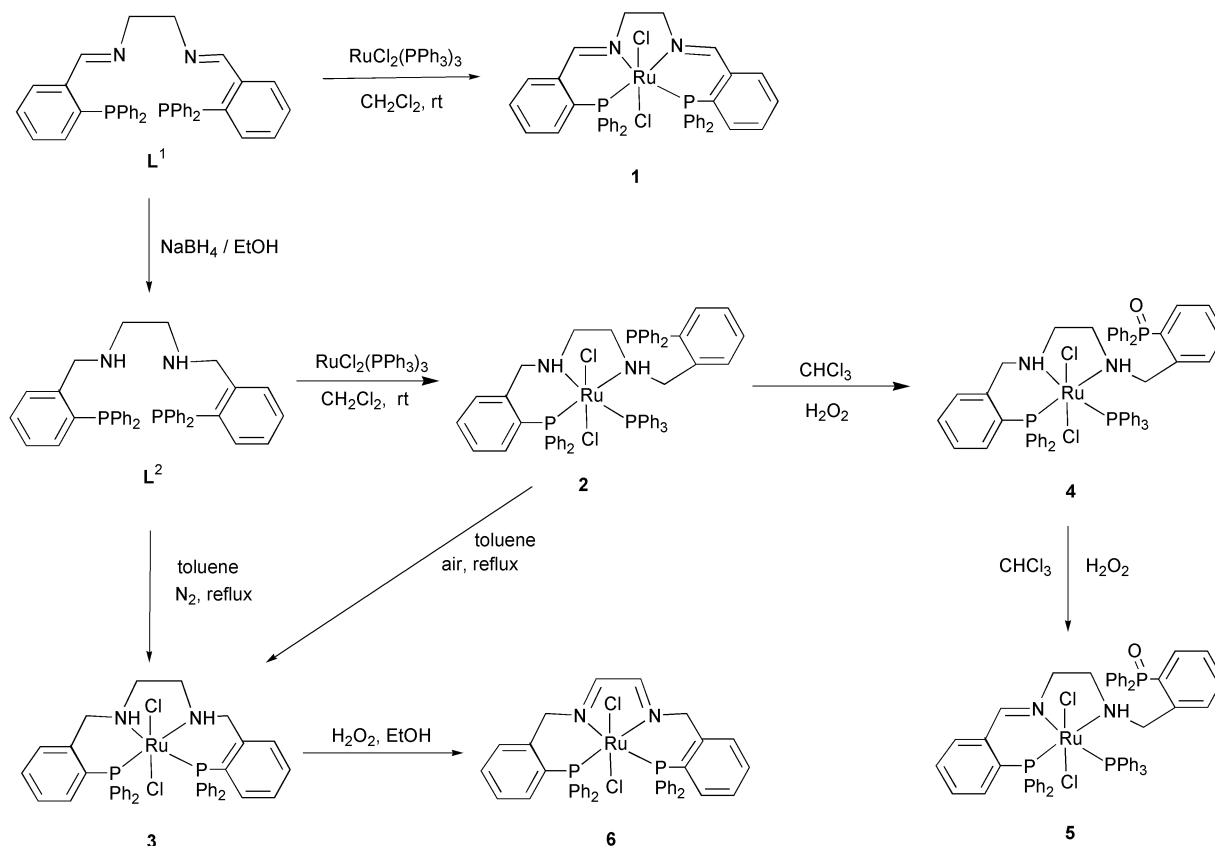


Chart 1



Scheme 1

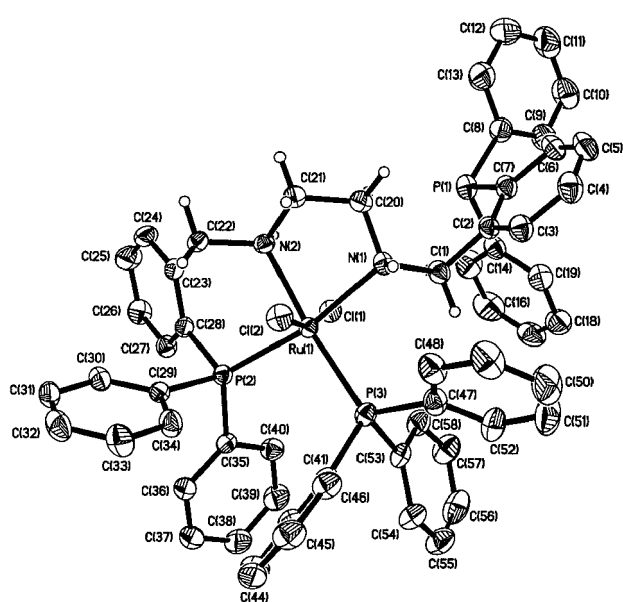


Fig. 1 A perspective drawing of compound **2**, with the atoms shown at the 30% probability level. Hydrogen atoms of all phenyl rings are omitted for clarity.

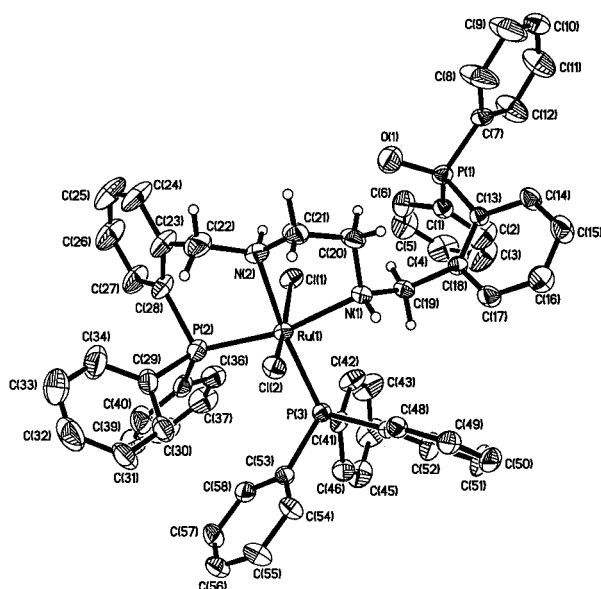
aminocyclohexane}.^{14,19} Selected bond lengths and bond angles of **2** are given in Table 1. Structural analysis revealed that the Ru atom adopts a slightly distorted octahedral geometry with a *trans*-RuCl₂ arrangement. The L² ligand acts as a tridentate ligand with a pendant PPh₂ group. The sixth site is occupied by a PPh₃ ligand, which is *cis* to the coordinated PPh₂ group of the L² ligand. The Ru–P, Ru–Cl and Ru–N distances are in the ranges expected for similar complexes of general formula RuCl₂[P(NH)(NH)P] [P(NH)(NH)P = L² and L⁶].^{10,12,14} The differences in the Ru–N [Ru(1)–N(1) 2.226(3), Ru(1)–N(2) 2.162(3) Å] and Ru–P [Ru(1)–P(2) 2.2987(9), Ru(1)–P(3)

2.346(1) Å] distances is a reflection of the chelate effect. The closing of the Cl(1)–Ru(1)–Cl(2) angle [165.9°(1)] reflects the steric crowding and chelate ring strain in the complex, as the chloro ligands are pushed away from the bulky PPh₃ toward the amino moiety *trans* to it. The spectroscopic data are consistent with the solid-state structure. The ³¹P{¹H} NMR spectrum of **2** exhibits two doublets and a singlet at δ 48.6 (d, ²J_{PP} = 28.9 Hz), 38.9 (d, ²J_{PP} = 28.9 Hz) and –13.3 (s) for P(2), P(3) and P(1), respectively, and its mass spectrum (positive FAB) shows a peak corresponding to its molecular ion (M + 1)⁺ at *m/z* 1042.

When refluxed in toluene in air, **2** lost the PPh₃ ligand to give *trans*-RuCl₂(κ⁴-L²) **3**, which could also be obtained by reacting L² with RuCl₂(DMSO)₄ in refluxing toluene.⁵ When reacted with excess H₂O₂ at room temperature, **2** was oxidized to a complex mixture. However, the degree of oxidation could be controlled by the amount of H₂O₂ added. When treated with one equivalent of H₂O₂, **2** was slowly oxidized to *trans*-RuCl₂(PPh₃)(κ³-L³) **4**. The progress of the oxidation was monitored by ³¹P{¹H} NMR spectroscopy. The pendant phosphine at δ –13.3 (s) was slowly converted to the phosphine oxide at δ 29.2 (s). This is further supported by the mass spectral data (positive FAB), which exhibits the molecular ion peak (M + 1)⁺ at *m/z* 1058, which is 16 mass units more than that of **2**. The structure of **4** was confirmed by X-ray crystallography (Fig. 2). Selected bond lengths and bond angles are given in Table 1. Structural analysis revealed that other than the pendant phosphine of the tridentate ligand κ³-L² being oxidized to the phosphine oxide, the structure of **4** is very similar to that of **2**. The Ru atom adopts a slightly distorted octahedral geometry with a *trans*-RuCl₂ arrangement and a Cl(1)–Ru(1)–Cl(2) angle of 166.3(1)°. The L³ ligand acts as a tridentate ligand with the PPh₂ group *cis* to PPh₃. The Ru–P, Ru–Cl and Ru–N distances are similar to those of **2**. The differences in the Ru–N [Ru(1)–N(1) 2.226(3), Ru(1)–N(2) 2.158(3) Å] and Ru–P [Ru(1)–P(2) 2.287(1), Ru(1)–P(3) 2.342(1) Å] distances is again a reflection of the chelate effect. The ³¹P{¹H} NMR spectrum of **4** is

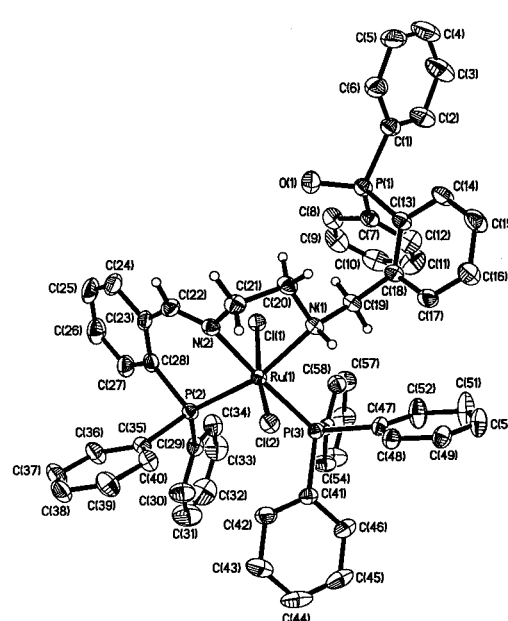
Table 1 Selected bond lengths (Å) and bond angles (°) for compounds **2**, **4**, **5** and **6**

Compound 2		Compound 4		Compound 5		Compound 6	
Ru(1)–P(2)	2.2987(9)	Ru(1)–P(2)	2.287(1)	Ru(1)–P(2)	2.273(1)	Ru(1)–P(1)	2.345(1)
Ru(1)–P(3)	2.346(1)	Ru(1)–P(3)	2.342(1)	Ru(1)–P(3)	2.357(1)	Ru(1)–P(2)	2.332(1)
Ru(1)–N(1)	2.226(3)	Ru(1)–N(1)	2.226(3)	Ru(1)–N(1)	2.228(2)	Ru(1)–N(1)	2.050(2)
Ru(1)–N(2)	2.162(3)	Ru(1)–N(2)	2.158(3)	Ru(1)–N(2)	2.073(3)	Ru(1)–N(2)	2.048(2)
Ru(1)–Cl(1)	2.4527(9)	Ru(1)–Cl(1)	2.416(1)	Ru(1)–Cl(1)	2.407(5)	Ru(1)–Cl(1)	2.407(8)
Ru(1)–Cl(2)	2.4191(9)	Ru(1)–Cl(2)	2.402(1)	Ru(1)–Cl(2)	2.438(9)	Ru(1)–Cl(2)	2.415(8)
N(1)–C(1)	1.497(4)	N(1)–C(19)	1.490(4)	N(1)–C(19)	1.483(4)	N(1)–C(19)	1.452(4)
N(1)–C(20)	1.501(5)	N(1)–C(20)	1.498(4)	N(1)–C(20)	1.487(4)	N(1)–C(20)	1.294(4)
N(2)–C(21)	1.483(5)	N(2)–C(21)	1.455(4)	N(2)–C(21)	1.463(4)	N(2)–C(21)	1.284(4)
N(2)–C(22)	1.489(4)	N(2)–C(22)	1.474(5)	N(2)–C(22)	1.273(4)	N(2)–C(22)	1.450(4)
		P(1)–O(1)	1.456(3)	P(1)–O(1)	1.488(3)	C(20)–C(21)	1.434(5)
P(2)–Ru(1)–P(3)	97.95(3)	P(2)–Ru(1)–P(3)	98.35(4)	P(2)–Ru(1)–P(3)	98.1(1)	P(1)–Ru(1)–P(2)	102.3(1)
P(2)–Ru(1)–N(1)	167.97(8)	P(2)–Ru(1)–N(1)	167.4(3)	P(2)–Ru(1)–N(1)	165.3(2)	P(1)–Ru(1)–N(1)	90.5(2)
P(2)–Ru(1)–N(2)	88.9(1)	P(2)–Ru(1)–N(2)	89.1(1)	P(2)–Ru(1)–N(2)	86.7(1)	P(1)–Ru(1)–N(2)	165.5(3)
P(2)–Ru(1)–Cl(1)	89.6(3)	P(2)–Ru(1)–Cl(1)	89.5(1)	P(2)–Ru(1)–Cl(1)	87.4(1)	P(1)–Ru(1)–Cl(1)	86.9(1)
P(2)–Ru(1)–Cl(2)	95.1(1)	P(2)–Ru(1)–Cl(2)	94.5(1)	P(2)–Ru(1)–Cl(2)	103.0(1)	P(1)–Ru(1)–Cl(2)	101.9(1)
P(3)–Ru(1)–N(2)	172.3(1)	P(3)–Ru(1)–N(2)	171.6(1)	P(3)–Ru(1)–N(2)	174.6(1)	P(2)–Ru(1)–N(1)	166.5(1)
P(3)–Ru(1)–Cl(2)	89.5(1)	P(3)–Ru(1)–Cl(2)	90.5(4)	P(3)–Ru(1)–Cl(2)	87.5(1)	P(2)–Ru(1)–Cl(2)	87.4(1)
Cl(2)–Ru(1)–N(1)	85.7(1)	Cl(2)–Ru(1)–N(1)	85.9(5)	Cl(2)–Ru(1)–N(1)	81.6(4)	Cl(2)–Ru(1)–N(1)	85.7(1)
Cl(2)–Ru(1)–N(2)	86.3(1)	Cl(2)–Ru(1)–N(2)	85.0(2)	Cl(2)–Ru(1)–N(2)	89.1(1)	Cl(2)–Ru(1)–N(2)	85.7(1)
Cl(2)–Ru(1)–Cl(1)	165.9(1)	Cl(2)–Ru(1)–Cl(1)	166.3(1)	Cl(2)–Ru(1)–Cl(1)	168.2(1)	Cl(2)–Ru(1)–Cl(1)	170.2(1)
N(1)–C(1)–C(2)	114.7(3)	N(1)–C(19)–C(18)	114.4(3)	N(1)–C(19)–C(18)	114.4(3)	N(1)–C(20)–C(21)	115.9(3)
N(2)–C(22)–C(23)	108.9(3)	N(2)–C(22)–C(23)	112.0(4)	N(2)–C(22)–C(23)	127.3(3)	N(2)–C(21)–C(20)	116.1(3)

**Fig. 2** A perspective drawing of compound **4**, with the atoms shown at the 30% probability level. Hydrogen atoms of all phenyl rings are omitted for clarity.

consistent with its solid-state structure, exhibiting two doublets and a singlet at δ 47.4 (d, $^2J_{\text{PP}} = 28.5$ Hz), 38.5 (d, $^2J_{\text{PP}} = 28.5$ Hz) and 29.2 (s) for P(2), P(3) and P(1), respectively.

When reacted with one equivalent of H_2O_2 , **4** could be further oxidized to form *trans*- $\text{RuCl}_2(\text{PPh}_3)(\kappa^3\text{-L}^4)$ **5**, whose structure was ascertained by X-ray crystallography (Fig. 3). Selected bond lengths and bond angles are given in Table 1. Structural analysis revealed that the amino group *trans* to the PPh_3 group is oxidized to an imino group. The N(1)–C(19) and N(2)–C(22) distances of 1.483(4) and 1.273(4) Å are consistent with a carbon–nitrogen single and double bond, respectively. The Ru atom adopts a slightly distorted octahedral geometry with a *trans*- RuCl_2 arrangement and a Cl(1)–Ru(1)–Cl(2) angle of 168.2(1)°. The Ru–N distances [Ru–N(1) 2.228(2), Ru–N(2) 2.073(3) Å] reflect that the imino nitrogen, N(2), is more tightly bound to the Ru centre than the amino nitrogen, N(1). The Ru–P distance of the PPh_2 group [Ru(1)–P(2) 2.273(1) Å] is shorter than that of the PPh_3 group [Ru(1)–P(3) 2.357(1) Å]. This may be a reflection of the chelate effect as well as the *trans*

**Fig. 3** A perspective drawing of compound **5**, with the atoms shown at the 30% probability level. Hydrogen atoms of all phenyl rings are omitted for clarity.

influence. The solid-state structure is consistent with the ^{31}P , ^1H and ^{13}C NMR, IR and MS data. The $^{31}\text{P}\{^1\text{H}\}$ NMR spectrum of **5** exhibits two doublets and a singlet at δ 55.5 (d, $^2J_{\text{PP}} = 29.1$ Hz), 32.2 (d, $^2J_{\text{PP}} = 29.1$ Hz) and 30.1 (s), which can be assigned to P(2), P(3) and P(1), respectively. The presence of the imino group is supported by the ^1H and $^{13}\text{C}\{^1\text{H}\}$ NMR, and IR spectra. Compound **5** shows a singlet at δ 8.60 (1H, s) for the proton and a singlet at δ 169.9 (s) for the carbon of the $-\text{CH}=\text{N}-$ group in its ^1H and $^{13}\text{C}\{^1\text{H}\}$ NMR spectra, respectively, and $\nu_{\text{C}=\text{N}}$ at 1631 cm^{-1} in its IR spectrum. The positive FAB mass spectrum exhibits the molecular ion peak $(\text{M} + 1)^+$ at m/z 1056. In this oxidizing step, only one C–N bond was oxidized to a C=N bond.

When reacted with an excess of NaBH_4 in ethanol, **1** was reduced to **3** in high yield.⁵ However, when treated with excess H_2O_2 , **3**, instead of converting back to **1**, was oxidized to a blue species, *trans*- $\text{RuCl}_2(\kappa^4\text{-L}^5)$ **6**, whose structure was also ascertained by X-ray crystallography (Fig. 4). Selected bond lengths

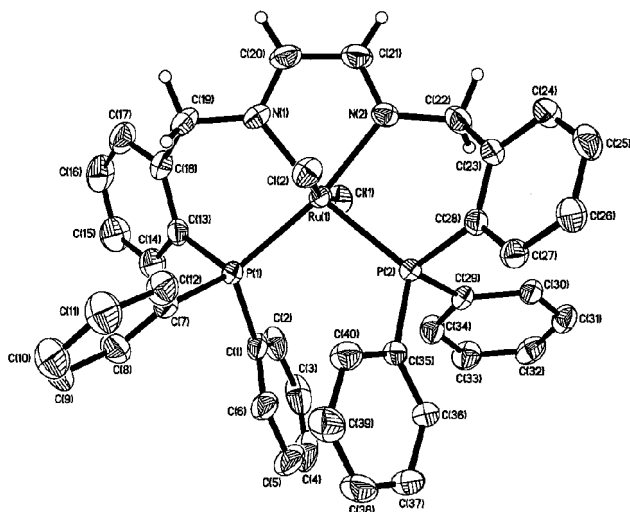


Fig. 4 A perspective drawing of compound **6**, with the atoms shown at the 30% probability level. Hydrogen atoms of all phenyl rings are omitted for clarity.

and bond angles are given in Table 1. Structural analysis revealed that the $[-N(H)CH_2CH_2N(H)-]$ diamino moiety is oxidized to a conjugated $(-N=CHCH=N-)$ diimino moiety. The $N(1)-C(20)$ and $N(2)-C(21)$ distances of 1.294(4) and 1.284(4) Å are consistent with carbon–nitrogen double bonds. The $C(20)-C(21)$ distance [1.434(5) Å] is slightly shorter than a normal carbon–carbon single bond, which is as expected for a conjugated $(-N=CHCH=N-)$ diimino moiety. Other than the diimino moiety, the structure of **6** is very similar to that of *trans*- $RuCl_2(\kappa^4-L)^1$.^{1,3} The Ru atom adopts a slightly distorted octahedral geometry with a *trans*- $RuCl_2$ arrangement and a $Cl(1)-Ru(1)-Cl(2)$ angle of 170.2(1)°. The Ru–N [Ru(1)–N(1) 2.050(2), Ru(1)–N(2) 2.048(2) Å] and Ru–P [Ru(1)–P(1) 2.345(1), Ru(1)–P(2) 2.332(1) Å] distances of **6** are slightly shorter than the Ru–N [Ru–N, 2.094(9) and 2.097(6) Å] and slightly longer than the Ru–P [Ru–P, 2.292(2) and 2.298(3) Å] distances of **1**, respectively.⁵ This is a reflection of the *trans* influence and the fact that a conjugated diimino group is a better π -acceptor than an isolated imino group. The solid-state structure is consistent with the ^{31}P , 1H and ^{13}C NMR, IR and MS data. The $^{31}P\{^1H\}$ NMR spectrum of **6** exhibits a singlet at δ 36.9 (s), which indicates the two phosphorus atoms are equivalent. The presence of the imino group is supported by the 1H and $^{13}C\{^1H\}$ NMR, and IR spectra. Compound **6** shows a singlet at δ 8.35 (s) for the proton and a singlet at δ 158.8 (s) for the carbon of the $(-N=CHCH=N-)$ moiety in its 1H and $^{13}C\{^1H\}$ NMR spectra, respectively, and $\nu_{C=N}$ at 1621 cm^{-1} in its IR spectrum. The positive FAB mass spectrum exhibits the molecular ion peak $(M + 1)^+$ at m/z 778.

Catalytic oxidation

The catalytic activities of compounds **1–5** to oxidize organic substrates with air have been examined. The results of the catalytic studies are summarized in Tables 2 and 3. Control experiments showed that oxidation of the organic substrates did not occur in the absence of the ruthenium complexes. Table 2 shows that at 80 °C, compounds **1–5** were all capable of catalyzing the oxidation of styrene to benzaldehyde and styrene oxide with air. The oxidations were non-selective, such that both epoxidation and oxidative cleavage of C=C bonds were observed. The ratio of benzaldehyde to styrene oxide was approximately 1 : 1 in all cases. Compound **2** showed the highest activity, with a conversion of 92% and a turnover frequency (TOF) of 1336. When we monitored the activity of **2** as a function of time, we found that the catalytic activity was preceded by an induction period of about 3 h. The formation of the products was not observed, even after 2.5 h, and a conver-

sion of only 0.32% was observed after 3.5 h. Then, a marked increase in catalytic activity was observed, with an overall conversion of 92% after 16 h. A similar observation was reported by Drago for the catalytic oxidation of norbornene with O_2 using *cis*- $[Ru(dmp)_2(CH_3CN)_2](PF_6)_2$ (*dmp* = 2,9-dimethyl-1,10-phenanthroline).²⁰ Drago proposed that the incubation period was due to the formation of a ruthenium peroxo norbornyl radical, which led to the formation of epoxide, alcohol and ketone. It is very likely that a similar mechanism is operative for **2**. When the catalytic reaction was carried out in the presence of a 100-fold excess of benzoquinone (a radical trap), no conversion was observed, even after 24 h. This supports the hypothesis that free radicals are present in the catalytic system. The reaction temperature, as well as the steric hindrance of the substituents on the aryl alkene, affects the catalytic activity of **2**. At 120 °C, **2** showed a higher activity; the conversion increased to 99%, the TOF increased to 2024 and the ratio of benzaldehyde to styrene oxide changed to approximately 1 : 2; however, at temperatures below 40 °C, no catalytic oxidation of styrene was observed. The activity of the catalytic oxidation of aryl alkenes decreases as the size of the substituents on the olefin increases. Thus, the conversion of α -methylstyrene to acetophenone and 2-phenylpropionaldehyde was only 26% (Table 3, entry 2), and no conversion was observed for *trans*-stilbene (Table 3, entry 3). The catalytic oxidation of **2** toward other organic substrates was also examined. Table 3 shows that **2** was able to catalyze the oxidation of *p*-tolualdehyde to 4-methylbenzoic acid (entry 4), 2-octanol to 2-octanone (entry 5) and benzyl alcohol to benzyl benzoate (entry 6).

The catalytic activity of **2** to oxidize organic substrates with *tert*-butyl hydroperoxide (TBHP) has also been studied (Table 4). In control experiments, no oxidized product was detected in the absence of either **2** or TBHP. Compound **2** catalyzed the oxidation of styrene with TBHP to benzaldehyde and styrene oxide (approximately 2 : 1 ratio, entry 1). However, with non-aryl alkene, the oxidations were more selective and proceeded mainly *via* epoxidation, with a much lower conversion. *cis*-Cyclooctene was oxidized to 9-oxabicyclo[6.1.0]nonane (entry 2) and norbornene to 2,3-epoxynorbornane (entry 3). Cyclohexene was oxidized to a mixture of 2-cyclohexen-1-ol and 2-cyclohexen-1-one (entry 4), however, the reaction was suppressed in the presence of 2,6-di-*tert*-butyl-4-methylphenol (entry 5). The observations that allylic oxidation was dominant over epoxidation and radical scavengers such as 2,6-di-*tert*-butyl-4-methylphenol suppressed the oxidation suggest that the catalytic reactions involve a free radical intermediate. This notion was further scrutinized by employing cumylhydroperoxide (CHP) as a mechanistic probe—cumyloxy radical, once formed, will undergo facile β -scission to form acetophenone and a methyl radical.²¹ When CHP was used as the oxidant, cyclohexene was oxidized to a mixture of 2-cyclohexen-1-ol and 2-cyclohexen-1-one with the formation of acetophenone, cumene and 2-phenyl-2-propanol.²² This strongly supports the hypothesis that the catalytic reaction operates *via* reactive alkoxy radicals. Compound **2** is also an efficient catalyst for the oxidation of alcohol with TBHP. In the presence of two equivalents of TBHP in benzene, **2** catalyzed the oxidation of primary alcohols to their corresponding acid (entry 6) or acid ester (entry 7), secondary alcohols to their corresponding ketones (entry 8 & 9) and phenol to *p*-benzoquinone (entry 10). Minisci *et al.* have reported that Fe(III) porphyrin catalyzes the oxidation of phenol to *p*-benzoquinone by TBHP *via* a free radical mechanism.²³ They found that the addition of pyridine enhanced the production of *p*-benzoquinone by catalyzing the decomposition of the alkylhydroperoxide intermediate. We used a similar strategy to test the involvement of reactive free radical species during catalysis and found that the rate of *p*-benzoquinone formation was higher when triethylamine was added to the reaction mixture (entry 11). This observation is consistent with Minisci's postulate.²³

Table 2 Catalytic oxidation of styrene with air using complexes **1–5**^a

Catalyst	Conv. (%) ^b	TOF/h ^{-1c}	Selectivity (%) ^d	
			Benzylaldehyde ^e	Styrene oxide ^e
1	23	320	56	44
2	92	1336	52	48
	99 ^f	2024	31	69
	0 ^g	0	0	0
3	25	363	41	59
4	51	741	51	49
5	22	319	56	44

^a The reactions were stirred in air at 80 °C for 16 h with the following conditions: catalyst, 0.001 mmol; styrene, 3 g. ^b Determined by GLC analysis based on the starting substrate using an internal standard. ^c TOF = mol of products/mol of catalyst per hour. ^d Determined by GLC analysis based on the converted substrate using an internal standard. ^e Identified by GC-MS. ^f At 120 °C. ^g At 40 °C.

Table 3 Catalytic oxidation of organic compounds with air using complex **2** as catalyst^a

Entry	Substrate	Conv. (%) ^b	Product ^c	Selectivity (%) ^d
1	Styrene	92	Benzylaldehyde	52
			Styrene oxide	48
2	<i>α</i> -Methylstyrene	26	Acetophenone	57
			2-Phenylpropionaldehyde	41
3	<i>trans</i> -Stilbene ^e	0	—	0
4	<i>p</i> -Tolualdehyde	57	4-Methylbenzoic acid	99
5	2-Octanol	5.6	2-Octanone	98
6	Benzyl alcohol	1.6	Benzyl benzoate	97

^a The reactions were stirred in air at 80 °C for 16 h with the following conditions: catalyst, 0.001 mmol; organic substrate, 3 g. ^b Determined by GLC analysis based on the starting substrate using an internal standard. ^c Identified by GC-MS. ^d Determined by GLC analysis based on the converted substrate using an internal standard. ^e 3 g of *trans*-stilbene was dissolved in 4 cm³ of *p*-xylene and 0.001 mmol of **2** was added. Then the mixture was stirred at 80 °C for 16 h.

Table 4 Catalytic oxidation of organic compounds with TBHP using complex **2** as catalyst^a

Entry	Substrate	Conv. (%) ^b	Product ^c	Selectivity (%) ^d
1	Styrene	84	Benzylaldehyde	62
			Styrene oxide	37
2	<i>cis</i> -Cyclooctene	29	9-Oxabicyclo[6.1.0]nonane	98
3	Norbornylene	19	2,3-Epoxybornane	97
4	Cyclohexene	26	2-Cyclohexen-1-ol	4
			2-Cyclohexen-1-one	93
5	Cyclohexene ^e	1.9	2-Cyclohexen-1-one	97
6	Benzylalcohol	88	Benzoic acid	97
7	3-Methyl-1-butanol	54	3-Methylbutyl 3-methylbutanoate	95
8	2-Octanol	96	2-Octanone	96
9	Cyclohexanol	75	Cyclohexanone	96
10	Phenol	17	<i>p</i> -Benzoquinone	94
11	Phenol ^f	28	<i>p</i> -Benzoquinone	96
12	Octane	4.4	2-Octanone	14
			4-Octanone	82
13	Cyclohexane	5.3	Cyclohexanol	19
			Cyclohexanone	72
14	Cyclohexane ^g	4.9	Cyclohexanol	15
			Cyclohexanone	74
			Cyclohexyl chloride	7
15	Adamantane	23	Adamantan-1-ol	93
			2-Adamantone	4
16	<i>n</i> -Propylbenzene	18	1-Phenyl-1-propanone	96
17	Ethylbenzene	48	Acetophenone	97
18	Diphenylmethane	47	Benzophenone	99
19	Cumene	68	2-Phenyl-2-propanol	93
			Acetophenone	5
20	1,3-Diisopropylbenzene	70	2,4-Diisopropylphenol	93

^a The reactions were stirred under nitrogen at room temperature for 16 h with the following conditions: catalyst, 0.001 mmol; organic substrate, 1.5 mmol; TBHP, 3.2 mmol; solvent, benzene, 3 cm³. ^b Determined by GLC analysis based on the starting substrate using an internal standard. ^c Identified by GC-MS. ^d Determined by GLC analysis based on the converted substrate using an internal standard. ^e 2,6-Di-*tert*-butyl-4-methylphenol (0.35 g, 1.6 mmol) was also added to the reaction mixture. ^f Triethylamine (0.09 mmol) was also added to the reaction mixture. ^g Solvent, benzene-CCl₄ 9 : 1.

Furthermore, **2** was capable of catalyzing the oxidation of unactivated saturated C–H bonds with TBHP. Alkanes were oxidized to either their corresponding ketones or alcohols, or a

mixture of both. The conversions were low for unsubstituted aliphatic alkanes, ranging from 4.4 to 5.3%. In the presence of two equivalents of TBHP and a catalytic amount of **2**, octane

was oxidized to a mixture of 2-octanone and 4-octanone (entry 12), cyclohexane to cyclohexanol and cyclohexanone (entry 13), and adamantane to adamantane-1-ol and 2-adamantone (entry 15). The fact that oxidation of octane occurred at the secondary C–H bond exclusively, with no detectable products from primary C–H bond oxidation, and adamantane preferentially at the tertiary C–H bond suggests that the alkane oxidations probably proceed *via* a H-atom abstraction pathway with rapid radical recombination. This is further supported by the oxidation of cyclohexane in a 9 : 1 benzene–CCl₄ mixture (entry 14), which gave cyclohexanol and cyclohexanone, as well as cyclohexyl chloride. A similar mechanism has been proposed for ruthenium-catalyzed oxidation of alkanes with TBHP.²⁴ However, the conversions for aryl-substituted alkanes were much higher, ranging from 18 to 70%. Under the same conditions, *n*-propylbenzene was oxidized to 1-phenyl-1-propanone (entry 16), ethylbenzene to acetophenone (entry 17), diphenylmethane to benzophenone (entry 18), cumene to a mixture of 2-phenyl-2-propanol and acetophenone (entry 19), and 1,3-diisopropylbenzene to 2,4-diisopropylphenol (entry 20). The substantial increase in the oxidation reactivity of **2** from octane to 1,3-diisopropylbenzene is consistent with the stability of the radicals generated through H-atom abstraction, *i.e.* aryl-substituted radicals are more stable than unsubstituted radicals. Experimental evidence suggests that free radicals are probably involved in the catalytic oxidation processes.

Experimental

General procedures

Unless otherwise stated, all reactions were carried out in an atmosphere of dry nitrogen or *in vacuo*. Solvents were dried by standard procedures, distilled and deaerated prior to use. All chemicals used were of reagent grade, obtained from the Aldrich Chemical Company and, where appropriate, degassed before use. Melting points were taken in sealed capillaries and are uncorrected. The compounds **L**¹, **L**²,⁷ and RuCl₂(PPh₃)₃²⁵ were prepared according to literature methods. Microanalyses were performed by the Shanghai Institute of Organic Chemistry, Chinese Academy of Sciences. The IR spectra (KBr pellets) were recorded on a Nicolet Magna-IR 550 spectrometer and NMR spectra on a JEOL EX270 spectrometer. ¹H and ¹³C{¹H} NMR chemical shifts were referenced to internal deuterated solvents and then recalculated to TMS (δ 0.00), ³¹P{¹H} NMR spectra were referenced to external 85% H₃PO₄. Low resolution mass spectra (LRMS) were obtained on Finnigan MAT SSQ-710 and MAT 95 spectrometers in FAB (positive ion) mode and reported as *m/z*. Gas chromatograms were obtained on a HP 5890 GC system or a HP 6890-5972 GC-MSD system. The progress of all the reactions was monitored by ³¹P{¹H} NMR spectroscopy.

Preparations

Synthesis of *trans*-RuCl₂(PPh₃)₃(κ³-L**²) **2**.** A solution of **L**² (0.060 g, 0.1 mmol) and RuCl₂(PPh₃)₃ (0.096 g, 0.1 mmol) in dichloromethane (30 cm³) was stirred at room temperature for 4 h, then the solvent was removed *in vacuo* to give an orange residue which was washed with *n*-hexane (2 × 5 cm³). The residue was purified by column chromatography. When eluting with chloroform, an orange band was obtained from the silica gel column. Removal of the solvent from the orange band gave an orange solid which, upon crystallization in a chloroform–hexane mixture, gave orange crystals of **2**. Yield: 0.087 g, 84%; m.p. 190–191 °C (dec). IR (cm^{−1}, in KBr): 3057m, 1568m, 1481m, 1432s, 1188m, 1087m, 975m, 746vs, 695vs and 520vs. NMR (CDCl₃): ³¹P{¹H}, δ 48.6 (d, ²*J*_{P-P} = 28.9 Hz, PPh₂), 38.9 (d, ²*J*_{P-P} = 28.9 Hz, PPh₃) and −13.3 (s, pendant PPh₂); ¹³C{¹H}, δ 126.7–141.5 (m), 57.0 (s), 49.2 (s), 31.9 (s) and 22.8 (s); ¹H, δ 6.41–7.99 (43H, m, Ph-H), 4.70 (2H, m, PhCH₂–), 4.32 (2H,

m, PhCH₂–), 3.61 (2H, m, –NCH₂CH₂N–), 3.30 (2H, m, –NCH₂CH₂N–), 2.80 (1H, m, NH), 2.51 (1H, m, NH) and 7.21 (0.75H, s, CHCl₃). Found (calc. for C₅₈H₅₃N₂P₃Cl₂Ru·0.75CHCl₃): C, 61.96 (62.27); H, 5.03 (4.75); N, 2.65 (2.47)%. LRMS (positive FAB) *m/z*: 1042 (M + 1)⁺ for ¹⁰²Ru and ³⁵Cl.

Synthesis of *trans*-RuCl₂(κ⁴-L**³) **3**.** A solution of **2** (0.035 g, 0.034 mmol) in toluene (20 cm³) was heated under reflux in air for 6 h. After cooling to room temperature, the solution was filtered and evaporated to dryness *in vacuo* to give an orange residue. The residue was washed with diethyl ether (2 × 5 cm³) and crystallized in a dichloromethane–*n*-hexane mixture to give orange crystals of **3**. Yield: 0.024 g, 92%. The identity of **3** was confirmed by comparing its IR, ³¹P{¹H} and ¹H NMR, and MS (positive FAB) data with those of an authentic sample of *trans*-RuCl₂(κ⁴-**L**³).⁵

Synthesis of *trans*-RuCl₂(PPh₃)₃(κ³-L**³) **4**.** A 30% solution of H₂O₂ (0.024 g, 0.212 mmol) was added dropwise to a solution of **2** (0.210 g, 0.202 mmol) in chloroform (30 cm³). The reaction mixture was stirred at room temperature for 12 h before it was filtered. The filtrate was evaporated to dryness *in vacuo* to give a red residue, which was washed with diethyl ether (2 × 5 cm³). Crystallization of the red residue in a chloroform–diethyl ether mixture gave red crystals of **4**. Yield: 0.198 g, 93%; m.p. 195–196 °C (dec). IR (cm^{−1}, in KBr): 3053m, 1481m, 1434s, 1197s, 1093m, 974m, 747s, 705s and 540s. NMR (CDCl₃): ³¹P{¹H}, δ 47.4 (d, ²*J*_{P-P} = 28.5 Hz, PPh₂), 38.5 (d, ²*J*_{P-P} = 28.5 Hz, PPh₃) and 29.2 [s, P(O)Ph₂]; ¹³C{¹H}, 126.4–133.6 (m), 49.9 (s), 45.4 (s), 31.4 (s) and 22.5 (s); ¹H, δ 6.21–7.70 (43H, m, Ph-H), 4.71 (2H, m, PhCH₂–), 4.38 (2H, m, PhCH₂–), 3.60 (2H, m, –NCH₂CH₂N–), 3.12 (2H, m, –NCH₂CH₂N–), 2.60 (1H, m, NH), 2.30 (1H, m, NH), 7.21 (1H, s, CHCl₃), 3.46 (4H, q, *J* = 6.8 Hz, CH₃CH₂O) and 1.15 (6H, t, *J* = 6.8 Hz, CH₃CH₂O). Found (calc. for C₅₈H₅₃Cl₂N₂OP₃Ru·CHCl₃·C₄H₁₀O): C, 60.33 (60.38); H, 5.13 (5.11); N, 2.31 (2.24)%. LRMS (positive FAB) *m/z*: 1058 (M + 1)⁺ for ¹⁰²Ru and ³⁵Cl.

Synthesis of *trans*-RuCl₂(PPh₃)₃(κ³-L**⁴) **5**.** A 30% solution of H₂O₂ (0.027 g, 0.238 mmol) was added dropwise to a solution of **4** (0.210 g, 0.198 mmol) in chloroform (30 cm³). The reaction mixture was stirred at room temperature for 12 h before it was filtered. The filtrate was evaporated to dryness *in vacuo* to give a red residue, which was washed with diethyl ether (2 × 5 cm³). Crystallization of the red residue in a chloroform–pentane mixture gave red crystals of **5**. Yield: 0.199 g, 95%; m.p. 200–201 °C (dec). IR (cm^{−1}, in KBr): 3048m, 1631m, 1481m, 1434s, 1186s, 1093m, 757s, 695s and 545s. NMR (CDCl₃): ³¹P{¹H}, δ 55.4 (d, ²*J*_{P-P} = 29.1 Hz, PPh₂), 32.2 (d, ²*J*_{P-P} = 29.1 Hz, PPh₃) and 30.1 [s, P(O)Ph₂]; ¹³C{¹H}, 169.9 (s), 126.9–134.6 (m), 59.8 (s), 30.9 (s) and 21.6 (s); ¹H, δ 8.60 (1H, s, –CH=N–), 6.21–7.52 (43H, m, Ph-H), 4.61 (2H, m, PhCH₂–), 4.40 (1H, m, –NCH₂CH₂N–), 3.60 (1H, m, –NCH₂CH₂N–), 3.31 (2H, m, –NCH₂CH₂N–), 2.60 (1H, m, NH), 7.22 (1H, s, CHCl₃) and 0.78–1.32 [12H, m(br), C₅H₁₂]. Found (calc. for C₅₈H₅₁Cl₂N₂OP₃Ru·CHCl₃·C₅H₁₂): C, 61.16 (61.51); H, 5.49 (5.14); N, 2.31 (2.25)%. LRMS (positive FAB) *m/z*: 1056 (M + 1)⁺ for ¹⁰²Ru and ³⁵Cl.

Synthesis of *trans*-RuCl₂(κ⁴-L**⁵) **6**.** To a yellow solution of **3** (0.180 g, 0.230 mmol) in a chloroform–ethanol mixture (20 cm³, 1 : 10), an excess of H₂O₂ (0.078 g, 0.617 mmol) was added. The progress of the reaction was monitored by ³¹P{¹H} NMR spectroscopy. After stirring at room temperature for 20 h, the reaction mixture turned purple. The solvent was removed to give a purple solid, which was re-dissolved in acetone and chromatographed on a silica gel column. A bright red band and a deep blue band were obtained when eluting with *n*-hexane–ethyl acetate (1 : 1) and ethyl acetate, respectively. Removal of the solvent from the red band gave a small amount of a red solid,

Table 5 Crystallographic data for compounds **2**, **4**, **5** and **6**

Compound	2 ·3CHCl ₃	4 ·H ₂ O	5 ·H ₂ O·0.25C ₆ H ₁₄	6 ·0.5H ₂ O·0.5CH ₃ OH
Empirical formula	C ₆₁ H ₅₆ Cl ₁₁ N ₂ P ₃ Ru	C ₅₈ H ₅₅ Cl ₂ N ₂ O ₂ P ₃ Ru	C _{59.5} H _{56.5} Cl ₂ N ₂ O ₂ P ₃ Ru	C _{40.5} H ₃₇ Cl ₂ N ₂ OP ₂ Ru
Formula weight	1401.01	1076.92	1096.44	801.63
Crystal size/mm	0.20 × 0.12 × 0.10	0.15 × 0.10 × 0.10	0.15 × 0.10 × 0.10	0.30 × 0.20 × 0.10
Crystal system	Triclinic	Monoclinic	Triclinic	Monoclinic
Space group	<i>P</i> $\bar{1}$	<i>P</i> 2 ₁ / <i>c</i>	<i>P</i> $\bar{1}$	<i>P</i> 2 ₁ / <i>c</i>
<i>a</i> /Å	12.590(1)	17.813(1)	14.6405(9)	20.124(2)
<i>b</i> /Å	12.833(1)	13.709(1)	14.7995(9)	18.343(2)
<i>c</i> /Å	21.502(2)	22.044(2)	16.0938(9)	10.1285(8)
<i>α</i> /°	93.614(2)	90	107.006(1)	90
<i>β</i> /°	100.712(2)	104.775(2)	100.158(1)	93.719(2)
<i>γ</i> /°	104.184(2)	90	112.860(1)	90
<i>V</i> /Å ³	3288.0(6)	5204.8(6)	2901.5(3)	3730.8(5)
<i>Z</i>	2	4	2	4
<i>D</i> _{calc} /g cm ^{−3}	1.415	1.372	1.249	1.422
<i>T</i> /K	293	293	293	293
Absorption coefficient/mm ^{−1}	0.797	0.540	0.486	0.683
<i>θ</i> range/°	1.71–26.00	1.77–27.51	1.40–27.54	2.03–27.51
Reflections collected	17759	30206	17170	21471
Independent reflections (<i>R</i> _{int})	12575 (0.0244)	11649 (0.0828)	12464 (0.0231)	8307 (0.0281)
Goodness-of-fit on <i>F</i> ²	0.994	0.784	0.986	1.046
Final <i>R</i> indices [<i>I</i> > 2σ(<i>I</i>)]	<i>R</i> 1 0.0516 <i>wR</i> 2 0.1450	0.0446 0.0741	0.0427 0.1125	0.0363 0.1030
<i>R</i> indices (all data)	<i>R</i> 1 0.0684 <i>wR</i> 2 0.1559	0.1449 0.0921	0.0661 0.1244	0.0534 0.1114

which was then discarded due to its extremely low yield. Removal of the solvent from the blue band gave a blue solid, which was recrystallized from a chloroform–hexane mixture to give deep blue crystals of **6**. Yield: 0.062 g, 35%; m.p 263–265 °C. IR (cm^{−1}, in KBr): 3053m, 1621(br)m, 1507m, 1429s, 1098m, 746m, 695s and 519s. NMR (CDCl₃): ³¹P{¹H}, δ 36.9 (s, PPh₂); ¹³C{¹H}, 158.8 (s), 127.3–134.8 (m) and 67.8 (s); ¹H, δ 8.35 (2H, s, –N=CHCH=N–), 6.98–7.27 (28H, m, Ph-H), 5.13 (4H, s, PhCH₂–), 7.21 (0.5H, s, CHCl₃) and 1.49 [4H, s(br), H₂O]. Found (calc. for C₄₀H₃₄Cl₂N₂P₂Ru·0.5CHCl₃·2H₂O): C, 55.52 (55.73); H, 4.42 (4.41); N, 3.41 (3.21)%. LRMS (positive FAB) *m/z*: 778 (*M* + 1)⁺ for ¹⁰²Ru and ³⁵Cl.

Catalytic studies

General procedure for catalytic oxidation by air. A reaction mixture of organic substrate (3.0 g) and catalyst (0.001 mmol) was stirred at 80 °C in air for 16 h. The resultant solution was analysed by GC. The identity of the analytes was verified by GC-MS. Control experiments without the catalyst were performed under identical conditions. The results of the catalytic studies are given in Tables 2 and 3.

General procedure for catalytic oxidation by TBHP. A solution of organic substrate (1.5 mmol), TBHP (3.2 mmol) and **2** (1 mg, 0.001 mmol) in benzene (3 cm³) was stirred under nitrogen at room temperature for 16 h. The reaction mixture was then poured slowly into a 10% aqueous Na₂SO₃ solution (5 cm³) to destroy any remaining TBHP and the resultant solution was extracted with dichloromethane. The organic layer was separated, dried over anhydrous Na₂SO₄ and analysed by GC. The identity of the analytes was verified by GC-MS. Control experiments without either the catalyst or TBHP were performed under identical conditions.

X-Ray crystallography

Pertinent crystallographic data and other experimental details are summarized in Table 5. Crystals of **2**·3CHCl₃, **4**·H₂O, **5**·H₂O·0.25C₆H₁₄ and **6**·0.5CH₃OH·0.5H₂O suitable for X-ray diffraction studies were grown by slow evaporation of **2** in a chloroform–hexane mixture, **4** in an acetone–diethyl ether mixture, **5** in an acetone–hexane mixture and **6** in a methanol–diethyl ether mixture, respectively. The water of crystallization probably came from the solvents, which were not dried prior to

use. The crystals were wrapped in epoxy glue to prevent them from losing solvent, and mounted on a thin glass fibre. No decay in intensity was encountered during the data collection. Intensity data were collected at 293 K on a Bruker Axs SMART 1000 CCD area-detector diffractometer using graphite-monochromated Mo-Kα radiation (λ = 0.71073 Å). The collected frames were processed with the software SAINT²⁶ and an absorption correction was applied (SADABS)²⁷ to the collected reflections. The structures of all compounds were solved by direct methods (SHELXTLTM)²⁸ and refined against *F*² by full matrix least-squares analysis. The presence of voids in the crystal lattices of **4** and **5** is presumably caused by the coincidentally inefficient packing of their respective molecules, which possess numerous bulky phosphino moieties. All non-hydrogen atoms were refined anisotropically. Except for the hydrogen atoms of the solvent molecules in **4**, **5** and **6**, which were not located, all other hydrogen atoms were generated in their idealized positions and allowed to ride on their respective parent carbon atoms.

CCDC reference numbers 169813–169816.

See <http://www.rsc.org/suppdata/dt/b1/b106997g/> for crystallographic data in CIF or other electronic format.

Acknowledgements

W.-K. W thanks the Hong Kong Baptist University and the Hong Kong Research Grants Council (HKBU 2053/97P) for financial support, and Prof. K. Y. Wong of Hong Kong Polytechnic University for helpful discussions and sharing some results prior to publication.

References

- W. K. Wong, J.-X. Gao, Z.-Y. Zhou and T. C. W. Mak, *Polyhedron*, 1992, **11**, 2965.
- W. K. Wong, J.-X. Gao and W. T. Wong, *Polyhedron*, 1993, **12**, 1647.
- W. K. Wong, J.-X. Gao, Z.-Y. Zhou and T. C. W. Mak, *Polyhedron*, 1993, **12**, 1415.
- W. K. Wong, J.-X. Gao, W. T. Wong, W. C. Cheng and C. M. Che, *J. Organomet. Chem.*, 1994, **471**, 277.
- J.-X. Gao, H.-L. Wan, W. K. Wong, M. C. Tse and W. T. Wong, *Polyhedron*, 1996, **15**, 1241.
- W. K. Wong, Y. Chen and W. T. Wong, *Polyhedron*, 1997, **16**, 433.
- J. C. Jeffrey, T. B. Rauchfuss and P. A. Tucker, *Inorg. Chem.*, 1980, **19**, 3306.

- 8 A. G. J. Ligtenbarg, E. K. van den Beuken, A. Meetsma, N. Veldman, W. J. J. Smeets, A. L. Spek and B. L. Feringa, *J. Chem. Soc., Dalton Trans.*, 1998, 263.
- 9 W. K. Wong, T. W. Chik, K. N. Hui, I. Williams, X. Feng, T. C. W. Mak and C. M. Che, *Polyhedron*, 1996, **15**, 4447.
- 10 W. K. Wong, T. W. Chik, X. Feng and T. C. W. Mak, *Polyhedron*, 1996, **15**, 3905.
- 11 W. K. Wong, L. L. Zhang, Y. Chen, W. Y. Wong, W. T. Wong, F. Xue and T. C. W. Mak, *J. Chem. Soc., Dalton Trans.*, 2000, 1397.
- 12 J. X. Gao, T. Ikariya and R. Noyori, *Organometallics*, 1996, **15**, 1087.
- 13 R. M. Stoop and A. Mezzetti, *Green Chem.*, 1999, 39.
- 14 R. M. Stoop, S. Bachmann, M. Valentini and A. Mezzetti, *Organometallics*, 2000, **19**, 4117.
- 15 S. Bachmann, M. Furler and A. Mezzetti, *Organometallics*, 2001, **20**, 2102.
- 16 B. M. Trost, *Acc. Chem. Res.*, 1996, **29**, 355.
- 17 G. C. Lloyd-Jones and S. C. Stephen, *Chem. Commun.*, 1998, 2321.
- 18 C. P. Butts, J. Crosby, G. C. Lloyd-Jones and S. C. Stephen, *Chem. Commun.*, 1999, 1707.
- 19 W. K. Wong, X.-P. Chen, W.-X. Pan, J.-P. Guo and W. Y. Wong, *Eur. J. Inorg. Chem.*, 2002, 231.
- 20 A. S. Goldstein, R. H. Beer and R. S. Drago, *J. Am. Chem. Soc.*, 1994, **116**, 2424.
- 21 D. W. Snelgrove, P. A. Macfaul, K. U. Ingold and M. D. D. Wayner, *Tetrahedron Lett.*, 1996, **37**, 823.
- 22 The reactions were stirred under nitrogen at room temperature for 16 h with the following conditions: catalyst, 0.001 mmol; organic substrate, 1.5 mmol; CHP, 3.2 mmol; solvent, benzene, 3 cm³.
- 23 A. Brovo, F. Fontana and F. Minisci, *Chem. Lett.*, 1996, 401.
- 24 C. M. Che, K. W. Cheng, M. C. W. Chan, T. C. Lau and C. K. Mak, *J. Org. Chem.*, 2000, **65**, 7996 and references therein.
- 25 S. J. La Placa and J. A. Ibers, *Inorg. Chem.*, 1965, **4**, 778.
- 26 SAINT Reference Manual, Siemens Energy and Automation, Madison, WI, 1994–1996.
- 27 G. M. Sheldrick, SADABS, Empirical Absorption Correction Program, University of Göttingen, Germany, 1997.
- 28 G. M. Sheldrick, SHELXTL™ Reference Manual, ver. 5.1, Siemens, Madison, WI, 1997.